Comparison of ^{99m}Tc-Methoxyisobutyl Isonitrile and ^{201}Tl Scintigraphy in Visualization of Suppressed Thyroid Tissue

Tanju Yusuf Erdil, Çetin Önsel, Bedii Kanmaz, Biray Caner, Kerim Sönmezoğlu, İsmail Çiftçi, Turgut Turoğlu, Levent Kabasakal, Haluk Burçak Sayman, and İlhami Uslu

Department of Nuclear Medicine, Marmara University School of Medicine, Istanbul; Department of Nuclear Medicine, Cerrahpaşa Medical Faculty, Istanbul University, Istanbul; and Department of Nuclear Medicine, Hacettepe University School of Medicine, Ankara, Turkey

Both ^{201}Tl and ^{99m}Tc-methoxyisobutyl isonitrile (MIBI) have been used in the visualization of suppressed thyroid tissue in patients with autonomously functioning thyroid nodules (AFTNs). It has been suggested that thyroid-stimulating hormone (TSH) control is not a major determinant of both tracers. However, the mechanism of thyroid uptake of these agents is controversial. In this study, we compared ^{201}Tl and MIBI in the visualization of suppressed thyroid tissue in patients with a solitary toxic AFTN. **Methods:** Thirty-two patients (13 triiodothyronine [T_3] and 19 T_3 + levorotatory thyroxine [T_4] hyperthyroid patients) with toxic AFTNs visualized on ^{99m}Tc-pertechnetate scanning were included in the study. All patients underwent MIBI and ^{201}Tl thyroid scintigraphy within a 3-d interval. The scintigrams were analyzed both visually and semiquantitatively. For the semiquantitative analysis, regions of interest (ROIs) were generated over the nodule (N) and contralateral normal lobe (E), and the mean counts in each ROI were calculated. **Results:** The N/E uptakes (mean ± SD) for pertechnetate, MIBI, and ^{201}Tl were 11.37 ± 4.53, 4.76 ± 1.38, and 1.63 ± 0.15, respectively, in T_3 + T_4 hyperthyroid patients and 9.46 ± 3.64, 2.73 ± 0.63, and 1.57 ± 0.23, respectively, in T_3 hyperthyroid patients. Our results showed that ^{201}Tl uptake of suppressed thyroid tissue compared with AFTN was more prominent and significantly higher than that of MIBI for both groups of patients (P = 1.08E-05 for T_3 and 6.15E-09 for T_3 + T_4 hyperthyroidism). There was no significant difference for either pertechnetate or ^{201}Tl ($P > 0.05$) when the N/E uptakes of both groups of patients were compared. However, the N/E uptake of MIBI in T_3 + T_4 hyperthyroid patients was significantly higher than that in T_3 hyperthyroid patients (P = 6.69E-06). **Conclusion:** Clear visualization of suppressed thyroid tissue with both ^{201}Tl and MIBI in patients with low serum concentrations of TSH suggests that TSH is not a major factor in the thyroid uptake of either agent. ^{201}Tl is superior to MIBI in the visualization of suppressed thyroid tissue in patients with a toxic thyroid nodule. An increased rate of metabolism in the follicular cells of AFTNs in T_3 + T_4 hyperthyroid patients compared with that in T_3 hyperthyroid patients might be responsible for the higher N/E for MIBI compared with that for ^{201}Tl.

Key Words: thyroid nodule; ^{99m}Tc-MIBI; ^{201}Tl; TSH

J Nucl Med 2000; 41:1163–1167

Received Jun. 16, 1999; revision accepted Oct. 27, 1999.

For correspondence contact: Tanju Yusuf Erdil, MD, Dikmen Cad. 123/9, Dikmen, Ankara, 06450 Turkey.

The solitary autonomously functioning thyroid nodule (AFTN) is a discrete nodular structure with function that is independent of pituitary control and unrelated to that of the remaining thyroid tissue (*1*). The molecular mechanism for the autonomous growth and function of these nodules has been related to mutations in the thyrotropin receptor that constitutively activate adenyl cyclase (*2*). Cyclic adenosine monophosphate stimulates the growth and differentiated thyroid function of the thyroid gland (*3*). Depending on the mass of hyperfunctioning tissue and related secretion of thyroid hormones, the patient may be euthyroid or hyperthyroid. However, most patients with AFTNs, whether manifest as a solitary nodule or as multiple nodules, will be euthyroid (*4,5*). If hyperthyroidism is present, the extranodular normal thyroid tissue is suppressed because of thyroid–pituitary axis feedback inhibition and is not visualized in conventional thyroid imaging using ^{131}I, ^{123}I, or ^{99m}Tc-pertechnetate (*1*). The presence of normal but suppressed thyroid tissue should be confirmed, and the functional relationship of the nodule and the normal thyroid tissue should be assessed so that radioactive iodine treatment or surgery can be performed with the confidence that suppressed thyroid tissue will subsequently function normally and hypothyroidism will not occur. To visualize the suppressed thyroid tissue, the thyroid-stimulating hormone (TSH; thyrotropin) stimulation test or sonography may be used (*6,7*). Sonography is a simple and convenient method to visualize thyroid tissue. However, it does not give any physiologic information. A lobe may be present but nonfunctioning for several reasons (*7*). In patients with hyperthyroidism, administration of TSH is potentially hazardous for the elderly and for patients with heart disease because of the potential release of thyroxine into the circulation, and bovine proteins may induce systemic or local allergic reactions (*8*). Furthermore, TSH is not commercially available in many countries. Because of these undesirable effects of TSH stimulation testing, both ^{201}Tl (*7,9*) and ^{99m}Tc-isonitrile complexes (*10–12*) have been used in the visualization of suppressed thyroid tissue. However, to our knowledge, no study has compared ^{201}Tl and ^{99m}Tc-

methoxyisobutyl isonitrile (MIBI) in the same patients. In this study, we compared ^{201}Tl and MIBI in the visualization of suppressed thyroid tissue in patients with a solitary toxic AFTN.

MATERIALS AND METHODS

Thirty-two patients (28 women, 4 men; age range, 23–72 y; average age, 51 y) with toxic AFTNs visualized on pertechnetate scanning were included in the study. Laboratory data were consistent with hyperthyroidism in all patients (TSH normal range, 0.4–5 μU/mL; triiodothyronine [T_3] normal range, 0.6–1.8 ng/mL; levorotatory thyroxine [T_4] normal range, 5–12 μg/dL). Thirteen patients had increased serum T_3 levels and normal serum T_4 levels (T_3 hyperthyroidism). In 19 patients, both serum T_3 and T_4 levels were increased (T_3 + T_4 hyperthyroidism). Our local ethical committee approved the study, and written informed consent was obtained from each patient.

First ^{201}Tl images (300 kcts) were obtained 15 min after intravenous injection of 80–100 MBq (2–3 mCi) tracer. Three days later, MIBI scanning was performed. Five hundred kilocounts were obtained 15 min after intravenous injection of 350–400 MBq (10–11 mCi) MIBI. An Orbiter ZLC 7500 gamma camera (Siemens Medical Systems, Hoffman Estates, IL) fitted with a high-resolution collimator was used. The images were taken on a 128 × 128 matrix. For MIBI, labeling efficiency was assessed by thin-layer chromatography and found to be >95% for all patients.

Every patient underwent sonography within 2 d of ^{99m}Tc-pertechnetate imaging using a real-time scanner with a 7.5-MHz transducer probe (RT-X 200; General Electric Medical Systems, Milwaukee, WI).

The scintigrams were analyzed both visually and semiquantitatively after normalization of both ^{201}Tl and MIBI images to pertechnetate images. For the semiquantitative analysis, regions of interest (ROIs) were generated over the AFTN, over the contralateral normal lobe, and 3 pixels below the right lobe of the gland (background), and the mean counts in every ROI were determined. Nodule-to-extranodular (N/E) uptake ratios were calculated for pertechnetate, ^{201}Tl, and MIBI after area correction for background activity by the following formula: (AFTN uptake − background)/(normal tissue uptake − background).

Statistical analysis was performed with the Student *t* test for comparison of T_3 and T_3 + T_4 hyperthyroid patients for each agent and with the paired Student *t* test for the comparison of the agents for each patient.

RESULTS

The results of the biochemical, scintigraphic, and statistical findings for each agent are summarized for all patients in Tables 1 and 2. ^{99m}Tc-pertechnetate scanning revealed a hot nodule with the suppression of the remaining thyroid tissue in all patients. Sonography revealed that that the mean volume of the nodules was 15.2 ± 6.1 cm^3, and most of the nodules showed cystic degeneration. In all patients, both ^{201}Tl and MIBI clearly visualized the suppressed thyroid tissue on pertechnetate scintigraphy (Figs. 1 and 2). For both T_3 and T_3 + T_4 hyperthyroid patients, ^{201}Tl uptake of suppressed thyroid tissue compared with AFTN was more prominent and significantly higher than that of MIBI (P = 1.08E-05 for T_3 and 6.15E-09 for T_3 + T_4 hyperthyroidism). There was no significant difference for either pertechnetate or ^{201}Tl ($P > 0.05$) when the N/E uptakes of T_3 and T_3 + T_4 hyperthyroid patients were compared. However, the N/E uptake of MIBI in T_3 + T_4 hyperthyroid patients was

TABLE 1
Biochemical and Scintigraphic Results in Patients with T_3 + T_4 Hyperthyroidism

Patient no.	Sex	Age (y)	T_3 (ng/mL) (0.6–1.8)*	T_4 (μg/dL) (5–12)*	TSH (μU/mL) (0.4–5)*	N/E uptake		
						^{99m}Tc-pertechnetate	MIBI	^{201}Tl
1	M	23	2.74	14.4	0.1	8.94	5.56	1.46
2	F	60	2.56	12.6	0.3	5.18	3.1	1.54
3	F	40	2.2	12.8	0.15	7.56	3.5	1.79
4	F	27	2.72	19.7	0.1	3.72	3.98	1.49
5	M	70	2.38	14.6	0.1	6.88	3.13	1.78
6	F	60	3.1	18.9	0.1	13.3	4.34	1.56
7	F	43	3.4	13	0.1	20.6	7.31	1.78
8	F	63	1.78	12.4	0.1	16.9	5.98	2.01
9	M	51	4.99	14.8	0.1	20.5	6.81	1.76
10	F	50	1.98	14.7	0.1	11.6	4.16	1.64
11	F	34	2.06	13.1	0.1	9.99	5.13	1.57
12	F	45	2.19	14.3	0.1	12.1	3.59	1.48
13	F	59	3.48	16.9	0.1	13.9	6.98	1.58
14	F	43	2.26	13.8	0.15	9.8	3.01	1.51
15	F	51	2.12	14.2	0.1	10.9	4.89	1.69
16	F	65	2.98	15.3	0.1	13.5	5.51	1.76
17	F	29	3.1	16.4	0.1	12.9	5.89	1.75
18	F	33	2.45	13.4	0.15	8.5	4.12	1.48
19	F	42	2.19	13.9	0.1	9.4	3.45	1.51
Mean ± SD		46.73 ± 13.75	2.66 ± 0.74	14.5 ± 1.69	0.11 ± 0.04	11.37 ± 4.53	4.76 ± 1.38	1.63 ± 0.15

*Values in parentheses are normal ranges.

TABLE 2
Biochemical and Scintigraphic Results in Patients with T_3 Hyperthyroidism

Patient no.	Sex	Age (y)	T_3 (ng/mL) (0.6–1.8)*	T_4 (μg/dL) (5–12)*	TSH (μU/mL) (0.4–5)*	N/E uptake		
						^{99m}Tc-pertechnetate	MIBI	^{201}Tl
1	F	42	1.97	8.7	0.15	18.7	2.72	1.71
2	F	53	1.89	7.1	0.3	6.1	2.79	1.45
3	F	72	1.83	11.2	0.18	6.91	1.43	1.24
4	F	65	1.98	11.9	0.3	6.03	2.11	1.64
5	F	43	1.97	9.9	0.3	6.87	3.58	1.46
6	M	24	2.13	10.9	0.15	10.6	3.8	1.89
7	F	48	1.99	10.5	0.15	7.93	2.94	1.49
8	F	55	1.96	9.6	0.18	6.45	2.45	1.39
9	F	32	1.91	10.9	0.15	9.98	2.78	1.95
10	F	59	2.03	11.1	0.15	11.9	3.01	1.59
11	F	63	2.04	11.3	0.15	8.91	2.73	1.91
12	F	41	2.09	11.2	0.15	13.7	3.21	1.33
13	F	51	1.97	9.1	0.15	8.9	2.06	1.39
Mean ± SD		49.84 ± 13.51	1.98 ± 0.08	10.26 ± 1.33	0.18 ± 0.06	9.46 ± 3.64	2.73 ± 0.63	1.57 ± 0.23

*Values in parentheses are normal ranges.

significantly higher than that in T_3 hyperthyroid patients (P = 6.69E-06).

DISCUSSION

In this study, both ^{201}Tl and MIBI clearly visualized the suppressed thyroid tissue in patients with solitary toxic AFTNs. The same results have been obtained by other investigators using ^{201}Tl (*7,9*), ^{99m}Tc-*t*-butyl isonitrile (*10*), and MIBI (*11,12*). ^{201}Tl is a monovalent cationic radioisotope with biologic properties similar to those of potassium (*13*). The low energy of ^{201}Tl results in significant scatter and attenuation, which impair image quality and lesion contrast. In addition, the slow clearance of ^{201}Tl from the body and the long physical half-life limit of the permissible injected dose result in count-deficient images. Waxman et al. (*14*) summarized the possible factors that influence ^{201}Tl uptake in tumor cells—i.e., blood flow, viability, tumor type, Na^+-K^+ adenosine triphosphatase system, $Na^+/K^+/2Cl^-$ cotransport system, Ca^{2+} ion channel system, vascular immaturity, and increased cell membrane permeability. Mayaan et al. (*15*) reported that ^{201}Tl was concentrated by a TSH-dependent process of active transport in mice thyroid. On the contrary, Iida et al. (*9*) and Corstens et al. (*7*) have shown that TSH was not a major determinant of ^{201}Tl uptake in the thyroid. Fukuchi et al. (*16*) did not find a correlation between thyroid function tests and ^{201}Tl uptake. Our study also showed that TSH control was not a major determinant of ^{201}Tl uptake because the suppressed thyroid tissue was clearly visualized even with very low TSH levels. However, McEvan et al. (*17*) reported a case in which the suppressed thyroid tissue was not visualized on ^{201}Tl scanning, but no clear explanation for this finding was given.

In comparison with ^{201}Tl, the ideal energy of MIBI results in less scatter and a shorter half-life allows a larger dose to be used without a higher radiation burden, resulting in a high photon flux and images of good quality. It is generally accepted that the uptake mechanism of MIBI involves passive diffusion across the plasma and mitochondrial

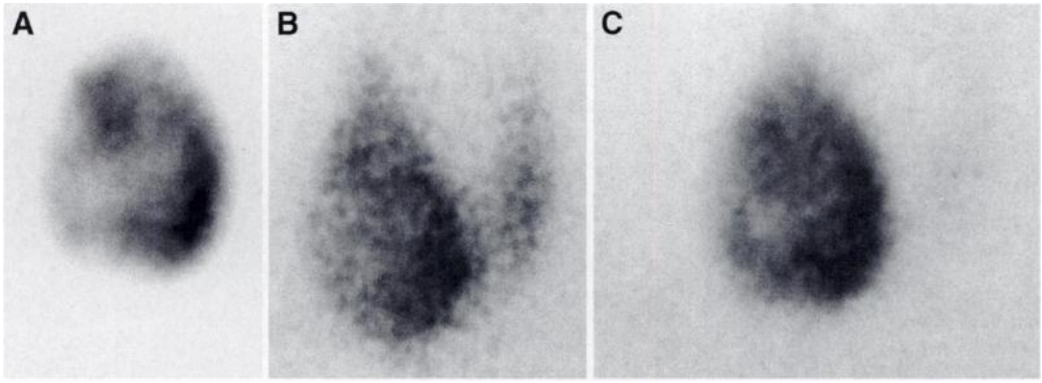

FIGURE 1. (A) ^{99m}Tc-pertechnetate image shows hyperactive nodule (N/E = 8.94) in right lobe of thyroid with complete suppression of left lobe in 23-y-old man (patient 1) with T_3 + T_4 hyperthyroidism. (B) ^{201}Tl scan clearly shows suppressed but normal left lobe (N/E = 1.46). (C) On ^{99m}Tc-MIBI image, left lobe is faintly visualized (N/E = 5.56).

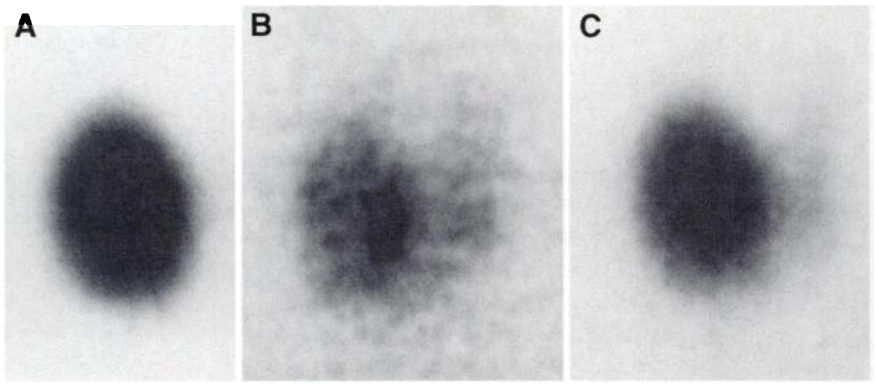

FIGURE 2. (A) ^{99m}Tc-pertechnetate image shows hyperactive nodule in right lobe of thyroid in 43-y-old woman (patient 5) with T_3 hyperthyroidism. Both ^{201}Tl scan (N/E = 1.46) (B) and ^{99m}Tc-MIBI image (N/E = 3.58) (C) clearly show suppressed thyroid tissue on ^{99m}Tc-pertechnetate image (N/E = 6.87).

membranes. At equilibrium, strong negative transmembrane potentials promote concentration of the agent within the inner matrix of the mitochondria (*18–20*). However, the thyroid uptake mechanism of MIBI is not clearly understood. Földes et al. (*21*) proposed that TSH and thyrotropin-releasing hormone administration caused a marked increase in thyroid uptake of MIBI in mice, whereas other investigators have reported that thyroid uptake of MIBI is not dependent on TSH stimulation (*11–12,22–24*). In our study, the clear delineation of suppressed thyroid tissue in patients with low serum concentrations of TSH suggests that TSH is not a major determinant of thyroid uptake of MIBI.

In this study, the suppressed thyroid tissue was more clearly delineated by visual analysis with ^{201}Tl than with MIBI, especially in patients with T_3 + T_4 hyperthyroidism. The uptake of ^{201}Tl in the suppressed thyroid tissue was more prominent semiquantitatively compared with that of AFTN and was significantly higher than that of MIBI in both groups. This finding might be related to greater MIBI uptake than ^{201}Tl uptake in the AFTN or greater ^{201}Tl uptake in the suppressed thyroid tissue than that of MIBI (or both). However, because we did not perform quantitative analysis, we could not determine the actual mechanism. In comparison of the N/E uptakes of T_3 and T_3 + T_4 hyperthyroid patients, ^{201}Tl showed no significant difference, whereas the N/E uptake of MIBI was significantly higher in T_3 + T_4 hyperthyroid patients than in T_3 hyperthyroid patients. This finding might be related to an increased metabolic activity and content of mitochondria in the follicular cells of the AFTN and higher metabolism-dependent uptake of MIBI compared with that of ^{201}Tl. Kao et al. (*25*) reported that MIBI showed increased uptake in the thyroid glands of patients with hyperthyroidism. It has been reported that the follicular cells in AFTNs contain abundant mitochondria (*26*), and >90% of MIBI is localized within the mitochondria (*27,28*), whereas >90% of ^{201}Tl is found in the soluble cytoplasmic fraction (*29*). Experiments in chick myocardial cells indicated that uptake and retention of MIBI are related to both mitochondrial metabolism and membrane potentials (*18,19,30*). It has been shown that metabolic derangement depresses uptake of the agent independent of blood flow (*31,32*).

According to our results, even though ^{201}Tl or MIBI uptake in the contralateral normal lobe signifies suppressed thyroid tissue in patients with solitary toxic AFTNs, both agents must be used carefully to show suppressed thyroid tissue in patients with toxic multinodular goiter. The patient might also have cold thyroid nodules or Graves disease superimposed on a multinodular goiter with cold nodules. Uptake can occur in tissue that has little or no iodine uptake at all (*22*). In these patients, ^{201}Tl or MIBI uptake may not signify suppressed thyroid tissue because cold nodules can also show intense ^{201}Tl and MIBI uptake (*33,34*).

CONCLUSION

Clear visualization of suppressed thyroid tissue with both ^{201}Tl and MIBI in patients with low serum TSH levels suggests that TSH is not a major determinant in the thyroid uptake of both agents. ^{201}Tl is superior to MIBI in the visualization of suppressed thyroid tissue in patients with toxic AFTNs, although ^{201}Tl has poor physical characteristics. An increased rate of metabolism in the follicular cells of AFTNs in T_3 + T_4 hyperthyroid patients compared with that in T_3 hyperthyroid patients might be responsible for the higher N/E uptakes for MIBI compared with those for ^{201}Tl.

ACKNOWLEDGMENTS

The authors thank Cavit Nişli for his technical assistance in performing imaging studies. This work was presented in part at the European Association of Nuclear Medicine Congress in 1994 in Düsseldorf, Germany.

REFERENCES

1. Hamburger JI. Solitary autonomously functioning thyroid lesions: diagnosis, clinical feature and pathogenetic considerations. *Am J Med.* 1975;58:740–748.
2. Tassi V, Di Cerbo A, Porcellini A, et al. Screening of thyrotropin mutations by fine-needle aspiration biopsy in autonomous functioning thyroid nodules in multinodular goiters. *Thyroid.* 1999;9:353–357.
3. Paschke R. Constitutively activating TSH receptor mutations as the cause of toxic thyroid adenoma, multinodular toxic goiter and autosomal dominant non autoimmune hyperthyroidism. *Exp Clin Endocrinol Diabetes.* 1996;104(suppl 4):129–132.
4. Hamburger JI. Evolution of toxicity in solitary nontoxic autonomously functioning thyroid nodules. *J Clin Endocrinol Metab.* 1980;50:1089–1093.
5. Hamburger JI. Should all autonomously functioning thyroid nodules be ablated to prevent the subsequent development of thyrotoxicosis? In: Hamburger JI, Miller JM, eds. *Controversies in Clinical Thyroidology.* New York, NY: Springer-Verlag; 1981:69.

6. Kammer H, Loveless MD. Disappearance of a hyperfunctioning nodule following TSH stimulation. *J Nucl Med.* 1978;19:1149–1150.
7. Corstens F, Huysmans D, Kloppenborg P. Thallium-201 scintigraphy of the suppressed thyroid: an alternative for iodine-123 scanning after TSH stimulation. *J Nucl Med.* 1988;29:1360–1363.
8. Krishnamurthy GT. Human reaction to bovine TSH. *J Nucl Med.* 1978;19:284–286.
9. Iida Y, Kasagi K, Misaki T, et al. Visualization of suppressed normal thyroid tissue by thallium-201 in patients with toxic nodular goiter. *Clin Nucl Med.* 1988;13:283–285.
10. Ramanathan P, Patel RB, Subrahmanyam N, et al. Visualization of suppressed thyroid tissue by technetium-99m-tertiary butyl isonitrile: an alternative to post-TSH stimulation scanning. *J Nucl Med.* 1990;31:1163–1165.
11. Kao CH, Lin WY, Wang SJ, et al. Visualization of suppressed thyroid tissue by Tc-99m MIBI. *Clin Nucl Med.* 1991;16:812–814.
12. Vattimo A, Bertelli P, Burroni L. Effective visualization of suppressed thyroid tissue by means of baseline Tc-99m-methoxy isobutyl isonitrile in comparison with Tc-99m pertechnetate scintigraphy after TSH stimulation. *J Nucl Biol Med.* 1992;36:315–318.
13. Gehring PJ, Hammand PB. The interrelationship between thallium and potassium in animals. *J Pharmocol Exp Ther.* 1967;155:187–201.
14. Waxman AD. Thallium-201 in nuclear oncology. In: Freeman LM, ed. *Nuclear Medicine Annual.* New York, NY: Raven; 1991:193–209.
15. Mayaan ML, Volpert EM, Fine EJ, et al. Thyroid uptake of thallium-201 and its control by TSH. *Acta Endocrinol (Copenh).* 1981;97:461–465.
16. Fukuchi M, Kido A, Hyoda A, et al. Uptake of thallium-201 in enlarged thyroid glands. *J Nucl Med.* 1979;20:827–832.
17. McEwan J, Park C. Nonvisualization of suppressed thyroid tissue on Tl-201 scintigraphy. *Clin Nucl Med.* 1993;18:950–952.
18. Chiu ML, Kronauge JF, Piwnica-Worms D. Effect of mitochondrial and plasma membrane potentials on accumulation of hexakis (2-methoxy-isobutylisonitrile technetium(I) in cultured mouse fibroblasts. *J Nucl Med.* 1990;31:1646–1653.
19. Delmon-Moinngeon LI, Piwnica-Worms D, Van den Abbeele AD, et al. Uptake of the cation hexakis (2-methoxyisobutylisonitrile)-technetium-99m by human carcinoma cell lines in vitro. *Cancer Res.* 1990;50:2196–2202.
20. Piwnica-Worms D, Holman LB. Noncardiac applications of hexakis (alkyl isonitrile) technetium-99m complexes. *J Nucl Med.* 1990;31:1166–1167.
21. Földes I. Effects of TSH on thyroidal 99-Tc MIBI accumulation [abstract]. *Eur J Nucl Med.* 1992;19:682.
22. Alonso O, Mut F, Lago G, et al. Tc-99m MIBI scanning of the thyroid gland in patients with markedly decreased pertechnetate uptake. *Nucl Med Commun.* 1998;19:257–261.
23. Osmanagaoglu K, Schelstraete K, Lippens M, et al. Visualization of a parathyroid adenoma with Tc-99m MIBI in a case with iodine saturation and impaired thallium uptake. *Clin Nucl Med.* 1993;18:214–216.
24. Muller SP, Piotrowsky B, Guth-Tougelides B, et al. Tc-99m MIBI and Tl-201 uptake in thyroid carcinoma [abstract]. *J Nucl Med.* 1988;29:854P.
25. Kao CH, Wang SJ, Liao SQ, et al. Quick diagnosis of hyperthyroidism with semiquantitative 30-min technetium-99m-methoxy-isobutyl-isonitrile thyroid uptake. *J Nucl Med.* 1993;34:71–74.
26. Goetsch E. Functional significance of mitochondria in toxic thyroid adenomata: preliminary report. *Johns Hopkins Hosp Rep.* 1916;27:129–133.
27. Crane P, Laliberte R, Heminway S, et al. Effect of mitochondrial viability and metabolism on technetium-99m-sestamibi myocardial retention. *Eur J Nucl Med.* 1993;20:20–25.
28. Carvallo PA, Chiu ML, Kronauge JF, et al. Subcellular distribution and analysis of technetium-99m-MIBI in isolated perfused rat hearts. *J Nucl Med.* 1992;33:1516–1521.
29. Mori K, Yamaguchi T, Maeda M. Mechanism of ^{201}thallium-chloride uptake in tumor cells and its relationship to potassium channels. *Neurol Res.* 1998;20:19–22.
30. Piwnica-Worms D, Kronauge JF, Chiu ML. Uptake and retention of hexakis (2-methoxyisobutyl isonitrile) technetium(I) in cultured chick myocardial cells: mitochondrial and plasma membrane potential dependence. *Circulation.* 1990;82:1826–1838.
31. Piwnica-Worms D, Kronauge JF, Delmon L, et al. Effect of metabolic inhibition on technetium-99m-MIBI kinetics in cultured chick myocardial cells. *J Nucl Med.* 1990;31:464–472.
32. Beller GA, Glover DK, Edwards NC, et al. Tc-99m-sestamibi uptake and retention during myocardial ischemia and reperfusion. *Circulation.* 1993;87:2033–2042.
33. El-Desouki M. Tl-201 thyroid imaging in differentiating benign from malignant thyroid nodules. *Clin Nucl Med.* 1991;16:425–430.
34. Nakahara H, Noguchi S, Nobuo M, et al. Technetium-99m-sestamibi scintigraphy compared with thallium-201 in evaluation of thyroid tumors. *J Nucl Med.* 1996;37:901–904.